Available online at www.sciencedirect.com
ScienceDirect
International Journal of Pharmaceutics 328 (2007) 22–34
INTERNATIONAL JOURNAL OF PHARMACEUTICS
www.elsevier.com/locate/ijpharm

Influence of particle wall adhesion on particle electrification in mixers

Kewu Zhu [a,*], Reginald B.H. Tan [a,b], Fengxi Chen [a], Kunn Hadinoto Ong [a], Paul W.S. Heng [c]

[a] *Institute of Chemical and Engineering Sciences, 1, Pesek Road, Jurong Island, Singapore 627833, Singapore*
[b] *Department of Chemical & Biomolecular Engineering, National University of Singapore, 4 Engineering Drive 4, Singapore 117576, Singapore*
[c] *Department of Pharmacy, National University of Singapore, 18 Science Drive 4, Singapore 117543, Singapore*

Received 1 April 2006; received in revised form 19 July 2006; accepted 25 July 2006
Available online 29 July 2006

Abstract

In this work, particle electrification in the Turbula and horizontally oscillating mixers were investigated for adipic acid, microcrystalline cellulose (MCC), and glycine particles. MCC and glycine particles acquired positive electrostatic charges, while adipic acid particles attained negative charges in both mixers. Adipic acid (of sieved size larger than 500 μm), MCC, and glycine particles were monotonically charged to saturated values, and had negligible wall adhesion. On the contrary, the adipic acid particles, both unsieved and sieved but of smaller sieved size fraction, exhibited very different charging kinetics in the horizontally oscillating mixer. These adipic acid particles firstly acquired charges up to a maximum value, and then the charges slowly reduced to a lower saturated value with increasing mixing time. Furthermore, these particles were found to adhere to the inner wall of the mixer, and the adhesion increased with mixing time. Surface specific charge densities for adipic acid particles were estimated based on particle size distribution, and were found to increase with particle mean diameters under the conditions investigated. The results obtained from the current work suggested that electrostatic force enhanced particle–wall adhesion, and the adhered particles can have a significant impact on particle electrification.

Keywords: Electrification; Adhesion; Mixer; Kinetics; Charge

1. Introduction

Electrostatic charges can be generated when two different materials are brought together and then separated (Harper, 1967). Particles can be charged when they are processed in gaseous environments. Particle electrification is commonly a nuisance and may cause dust explosions (Joseph and Klinzing, 1983; Jones, 1995). On the other hand, particle electrostatic charges can also be exploited for example in powder flow measurement (Masuda et al., 1998; Rosales et al., 2002), powder separation (Yanar and Kwetkus, 1995), electrophotography in photocopiers and laser printers, and dry powder coating (Kleber and Makin, 1998). For the safe operation of particle handling systems and optimization of the performance of particulate systems, it is of great importance to understand the particle electrification behavior in particle processing systems.

The mechanism for contact electrification is not well understood especially for electrification involving insulators. Diaz and Fenzel-Alexander (1993) presented an ion transfer model to described contact charging between polymer containing ions and another polymer or metal, and they suggested that the sign and magnitude of the charge depended on ion content in the surface region of the polymer, the relative mobilities of the two ions in the salt, and the relative stabilities of the two ions on each of the two surfaces in contact. Diaz and Felix-Navarro (2004) constructed a semi-quantitative tribo-electric series for polymer materials by combining data from literature with their quantitative charging results with metal contacts. In addition to ion transfer model, electron transfer mechanism has also been proposed to explain insulator metal charging systems. Castle and Schein (1995) suggested a surface state model (one of the electron transfer models) for the toner-carrier charging experiments and showed that majority of the data agreed with this model. Yu and Watson (2001) proposed a two-step electron transfer model to explain charging accumulation processes, namely contact of two surfaces and their separation. According to this model, interface states were formed and electrons from both surfaces were

* Corresponding author. Tel.: +65 6796 3861; fax: +65 6316 6183.
E-mail address: Zhu_Kewu@ices.a-star.edu.sg (K. Zhu).

0378-5173/$ – see front matter © 2006 Elsevier B.V. All rights reserved.
doi:10.1016/j.ijpharm.2006.07.041

Nomenclature

A	particle surface area (m^2)
d	particle diameter (m)
f	frequency
k	elasticity parameter (Pa^{-1})
k_c, k_0, k_r	constants
M	total mass (kg)
n	number of contacts
N	number of particles
p	number-based particle size distribution function (−)
q	single particle charge (C)
Q	total charge (C)
S	contact area (m^2)
t	time (s)
T	charge mass ratio (C/g)
v_i	particle impact velocity (m/s)
Z_0	gap between contact body (m)

Greek letters

ε	relative permittivity of air
ε_0	permittivity of vacuum ($C^2\ N^{-1}\ m^{-2}$)
θ	particle wall coverage
ρ	particle density (kg/m^3)
σ	surface specific density (C/m^2)
τ	time constant (s)
ϕ	contact potential difference (V)

distributed in this interface states when the contact was established. These electrons would redistribute during separation before the interface states were eliminated. This electron redistribution led the insulator to be negatively or positively charged depending on more or fewer electrons being transferred to the insulator. The charging continued via the two-step process until the equilibrium was reached. Clint and Dunstan (2001) showed that there was a good correlation between the electron-donor surface tension parameter and the position of the solid in the tribo-electric series, and they believed that contacting charging was due to the transfer of electrons rather than ions. Lee (1994) proposed a dual mechanism of contact electrification for metal-insulator system, which included both ion and electron charge transfer. How and why charge transfers are not known exactly (Matsusyama and Yamamoto, 2006). A simple condenser model has been commonly used in the discussion of powder electrification (Matsusyama and Yamamoto, 2006; Matsusaka et al., 2000; Masuda et al., 1976).

Many naturally observed phenomena such as radio noise, light emission, and singing/booming sands may be attributed to the electrical charges generated on naturally occurring particles in sand, silt and dust during transport (Kanagy and Mann, 1994). These generated electric charges may in turn greatly influence on the transport and deposition behavior of sand and slits (Zheng et al., 2003; Kanagy and Mann, 1994; Zheng et al., 2006). In the chemical and pharmaceutical industry, particle electrification has been associated with solid handling processes such as in the powder pneumatic conveying (Kanazawa et al., 1995; Zhu et al., 2004), gas–solid fluidized bed (Chen et al., 2003; Rasanen et al., 2004), melt agglomeration process (Eliasen et al., 1999), and inhalation device (Dubus et al., 2003; Kwok et al., 2005). Electrostatic charges can greatly alter the particle flow dynamics and, hence, the system performance. Electrostatic charges generated in a pneumatic conveying line were found to result in solid granules sticking to the wall of the conveying pipe and forming stationary capsule annular films (Zhu et al., 2004). The presence of electrostatic charges in a gas phase fluidized bed polymerization reactor influenced the reactor hydrodynamics such as bubble characteristics and particle mixing behavior, and the resultant electrostatic force eventually led to the formation of the wall sheet, which resulted in plugging of the reactor product discharge system or loss of fluidization (Hendrickson, 2006). Guardiola et al. (1996) investigated the influence of particle size, fluidization velocity, and relative humidity on the electrostatic charge generation and accumulation in a fluidized bed by means of potential difference using an electrical probe. They found that the degree of particle electrification increased with particle size and air velocity. They also pointed out that the effect of relative humidity on electrostatic charge was complex and depended on the quality of fluidization. The aforementioned studies suggested that, as a result of particle–particle and particle–wall collisions, particles were always charged in the handling system, and these electrostatic charges greatly influenced the performance of the handling system and subsequent processes involving these charged particles. However, most of the previous work has focused on particle electrification in gas–solid two-phase flows.

Byron et al. (1997) measured the fine powder dose charge (FPD charge) of aerosolized drug and lactose particles from Turbohaler™ and Dryhaler™. Their results suggested that the charge level of fine particle dose was too large to be neglected, and the electrostatic charge would not only affect the total and regional deposition in the human lung but also influence the aerosol dispersion behavior in the air stream. Kulvanich and Stewart (1987) explored the influence of storage time on the total adhesion force of drug-carrier interactive systems at the relative humidity of 33%. Their results showed that total adhesion force decreased with storage time up to 23 days, and they attributed the decrease of adhesion force to the decay of electrostatic charges. Influence of electrostatic charges on the amount of particle respiratory fraction was also demonstrated by Philip et al. (1997). These studies highlighted the importance of electrostatic charges in the inhalation drug delivery systems. The electrostatic charge not only affected the aerosol dispersion efficiency, but can also influenced the drug deposition behavior in the lung as well.

Mixing of particles is important in many pharmaceutical operations. In many situations, a better mixing process could tremendously increase the quality of product. In the formulation of dry powder inhalation product, mixing is regarded as a key process for preparing fine drug particles with coarse carrier particles to form a homogeneous mixture. Even the sequence of

adding mixing components was reported to have a significant impact on the performance of their final formulation product for inhalation drug delivery (Zeng et al., 1999). Electrostatic charges are generated and accumulated as a result of continuous collisions between particles and mixer container as well as between particles. The generated electrostatic charges affect binding between particles and the container wall as well as between particles, and hence influence the quality of final products. However, charge generation and accumulation during particle mixing is still not clear.

Understanding charge generation and accumulation processes in particle mixers is therefore very important in optimizing the mixing process and to improve the quality of formulation for dry powder inhalation drug delivery. Particle electrification is influenced by particle characteristics such as particle size, shape (Carter et al., 1998), purity and roughness, and the electrical and mechanical properties of particles and contact surfaces (Elsdon and Mitchell, 1976; Bailey and Smedley, 1991). Environmental conditions such as temperature and relative humidity are also known to affect charge generation and dissipation.

In the current work, particle electrification of adipic acid, microcrystalline cellulose (MCC), and glycine particles in a T2F Turbula mixer (Switzerland) was investigated. Electrostatic charges generated in the mixer operated at various rotation speeds and relative humidity were measured. Electrostatic charges were also measured in a horizontally oscillating mixer for these particles to investigate the influence of mixer operation mode on the electrostatic charge generation. Further experiments were carried out to investigate the influence of particle size on the particle electrification in the mixers. The purpose of the current work is to understand the charging kinetics of particles in the mixer, and to investigate the impact of operating condition, particle characteristics, mixer type, as well as relative humidity influence on the particle electrification.

2. Materials and methods

Adipic acid (Lot No: S11343-124) and MCC (Batch #07021PA) purchased from Sigma–Aldrich were used as supplied. Glycine was re-crystallized from aqueous solution by a cooling method. Adipic acid sample was mechanically sieved into six different size fractions as follows: *a*, >500 μm; *b*, 250–500 μm; *c*, 180–250 μm; *d*, 150–180 μm; *e*, 125–150 μm; *f*, 90–125 μm. MCC particles of particle size larger than 125 μm were also obtained from the purchased samples by mechanically sieving out the fines.

2.1. Particle characterization

Particle size distribution was measured with a laser diffraction technique (Malvern Mastersizer 2000, Malvern Instruments, UK) with a dry dispersion method. The dispersion pressure for dispersing particles was set to a value such that the measured particle size distribution did not vary further with increased dispersion pressure. Each of the measurements was repeated at least thrice with fresh samples to ensure reproducibility. Particle morphology was examined using the scanning electron microscope (SEM: model JSM-6700F, JEOL, USA). Particle images were also taken using an optical microscope, and the number-based particle size distribution was analyzed subsequently. Number-based particle geometric diameter distribution was also measured with time of flight technique using PSD 3603 (TSI, USA) to confirm the accuracy of the number-based distribution obtained from optical image analysis. True and bulk particle densities of the three samples were determined using Ultrapcynometer 1000 (Quantachrome, USA) and autotap density meter (Auantachrome, USA), respectively.

2.2. Charge measurement

The mixer container was made of a cylindrical stainless steel tube. During an experiment, the bottom cap of the container was fixed, while the top cap was removable for powder loading/unloading. A knob made of electric insulating material was attached to the container to minimize the electrostatic disturbance during the transport of the container. Precautions were taken to clean the mixer container well before conducting any experiment. Prior to each measurement the inner wall of the stainless steel container was washed with deionized water, scrubbed with a metal brush, rinsed with pure ethanol, and then blow dried using compressed air. The container was then placed in the humidity chamber to equilibrate at the environment conditions desired for the next experiment.

All the experiments were carried out in the controlled environmental chamber with the temperature set at 25 °C. A Faraday cage was used to measure electrostatic charges carried by powders through a charge induction method. The Faraday cage was placed within the environmental chamber, and connected to an electrometer (Keithley 6517, Keithley Instruments, USA) which was then connected to a computer through a GPIB interface. Fig. 1 presents the schematic diagram of experimental setup. The electrometer was switched on for at least 2 h before conducting experiments to minimize any electrical drifting. Powder samples were laid out as thin layers on earthed metal plates to equilibrate inside the environmental chamber (Model 518, ETS, USA) at the temperature of 25 °C and chosen relative humidity for at least 48 h before experimentation. A measured quantity of powder was loaded into the container with a spatula made using insulating material. The container was sealed with the top cap and mounted on the T2F Turbula mixer. After mixing for the required duration, the mixer was stopped, the container was removed, and powder was poured into the Faraday cage to measure the particle charges. The weight of particles inside the Faraday cage was measured and the specific charge (nC/g) was then calculated. Particles adhering to the container wall were also estimated from the difference in weights of powder originally loaded and that received in the Faraday cage.

The experimental procedure for measuring electrostatic charges of adipic acid, MCC, and glycine particles in the T2F Turbula mixer was carried out as previously described and for various mixing durations. The runs were continued until the measured specific charge did not change with further increasing in mixing time. Experiments were repeated to explore the influ-

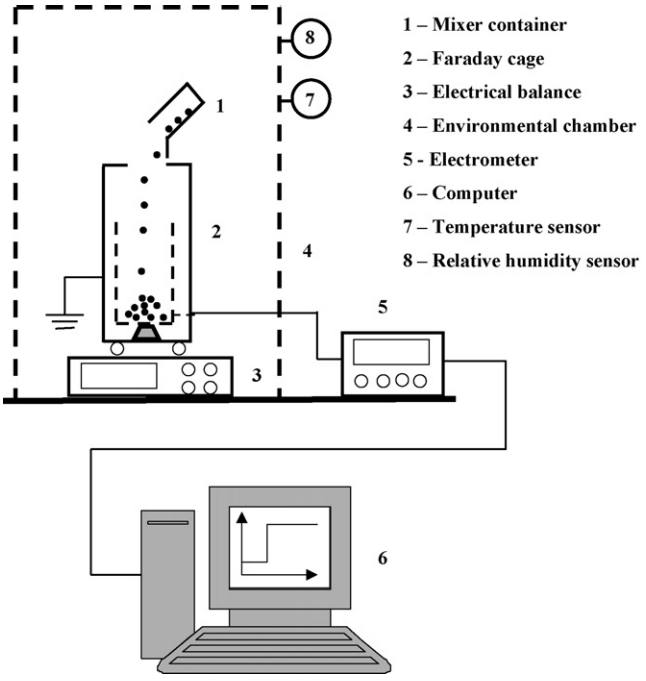

Fig. 1. Schematic diagram of experimental setup for measuring electrostatic charges.

ence of mixer rotation speed and relative humidity on particle electrification.

In addition to the Turbula mixer, particle electrification tests in a horizontally oscillating mixer for adipic acid, MCC, and glycine particles were also conducted. In contrast to the 3D motion in the Turbula mixer, the horizontally oscillating mixer has a lever of 30 cm with a sample holder at the top end for attaching the mixer container, and the bottom end is fixed to an axis which rotates at the frequency of 2.5 Hz and the rotation angle of 45°. Fig. A.1 (appendix) shows the schematic diagram of the mixer. The experimental procedure for the electrostatic charge measurement was the same as that for the Turbula mixer.

Particle charging characteristics of different size fractions was studied for adipic acid particles in the stainless steel mixer container operated with both the Turbula and the horizontally oscillating mixers.

3. Theoretical

A particle acquires a certain amount electrostatic charges if it collides with a metal plate and separates subsequently, leaving the plate with the same amount charges but of the opposite polarity. Charge transfer is a result of the potential difference between the two contact bodies. The potential difference is due to: (1) difference in surface work function of the contact bodies, and (2) potential difference arising from image charges (Masuda et al., 1976). Particle charges are also lost by dissipation toward the surrounding atmosphere with time. First order particle contact charging kinetics has been used to describe the impact charging between polymer and metal (Matsuyama and Yamamoto, 1995; Matsusaka et al., 2000). The total charges retained at the particle surface are the result of the two combined effects—charge transfer and charge relaxation, and it can be described using the following equation:

$$\frac{\mathrm{d}q}{\mathrm{d}n} = k_\mathrm{c}\frac{\varepsilon\varepsilon_0 S}{Z_0}(\phi - k_0 q) - \frac{k_\mathrm{r}}{f}q \tag{1}$$

where q is the particle charge; k_c, k_r, and k_0 the constants; ε the relative permittivity of air and ε_0 the permittivity of the vacuum; S the contact area; Z_0 the gap between contact bodies; f the contact frequency; n the contact number; and ϕ is the contact potential difference. The first term in the right-hand side of Eq. (1) represents charge generation after one particle–wall contact, which is function of the difference between contact potential difference (ϕ) and image charge potential difference (k_0q). The second term in the right hand side of Eq. (1) is charge dissipation in the time interval between successive contacts.

If the particle is assumed to be spherical with a diameter d and uniformly charged with surface charge density σ, particle charges become:

$$q = \pi d^2\sigma \tag{2}$$

For a period of time dt, the contact number is

$$\mathrm{d}n = f\,\mathrm{d}t \tag{3}$$

Substituting Eqs. (2) and (3) into Eq. (1):

$$\frac{\mathrm{d}\sigma}{\mathrm{d}t} = fk_\mathrm{c}\frac{\varepsilon\varepsilon_0 S}{Z_0}\left(\frac{\phi}{\pi d^2} - k_0\sigma\right) - k_\mathrm{r}\sigma \tag{4}$$

Integration Eq. (4) with initial condition ($t=0$, $\sigma=\sigma_0$), the following equation is obtained:

$$\sigma = \sigma_0\,\mathrm{e}^{-t/\tau} + \sigma_\infty(1 - \mathrm{e}^{-t/\tau}) \tag{5}$$

$$\tau = \left(\frac{fk_0k_\mathrm{c}\varepsilon_0\varepsilon S}{Z_0} + k_\mathrm{r}\right)^{-1} \tag{5.1}$$

$$\sigma_\infty = \frac{(1/\pi d^2)\phi}{k_0 + k_\mathrm{r}Z_0/fk_c\varepsilon_0\varepsilon S} \tag{5.2}$$

$$S = 1.36k^{2/5}\rho^{2/5}d^2v_i^{4/5} \tag{5.3}$$

Considering a powder sample having mass m, number probability $p(d)$ for particles having diameter d, and particle density ρ obtaining electrostatic charges due to continuously colliding with the stainless steel container wall of the mixer. If the volume of the powder is very small compared to that of the container, collisions between particles may be negligible. Particle–wall collisions are assumed to be random, and unhindered by the presence of other particles. In this case, the single particle–wall contact electrification equation (5) can be applied independently to each particle for the particle–wall contact electrification. If collisions between particles cannot be neglected, charges can be transferred not only during particle–wall collisions but also during particle–particle contacts. However, charge transfer between particles only results in charge redistribution among particles, and statistically will not affect overall particle wall charge behavior provided that no particle adheres to the wall. For example, saturated charges obtained will only be determined by the charging characteristics of particle–wall system and charge

relaxation process which is affected by the environmental conditions. Hence in the latter case the previous single particle–metal contact electrification results can still be applied to analyze particle electrification in the mixer. The first order charging kinetics described in Eq. (5) was shown to successfully analyze particle charging in the pneumatic conveying of solids (Matsusaka et al., 2003).

In real experiments, instead of charges carried by single particle, specific charge density (charge mass ratio) T is normally measured as follows:

$$T = \frac{Q}{M} \tag{6}$$

Assuming particles are uniformly charged with equal surface charge density σ, then total powder charges and the corresponding particle mass can be calculated as

$$Q = \int_0^\infty N\pi x^2 \sigma p(x)\,\mathrm{d}x \tag{7}$$

$$M = \int_0^\infty N\frac{1}{6}\pi x^3 \rho p(x)\,\mathrm{d}x \tag{8}$$

Substitute Eq. (7) and (8) into Eq. (6), and rearranging it:

$$\sigma = \frac{T\rho}{6}\left(\frac{\int_0^\infty x^3 p(x)\,\mathrm{d}x}{\int_0^\infty x^2 p(x)\,\mathrm{d}x}\right) \tag{9}$$

Surface charge density can be estimated from charge mass ratio and number-based particle size distribution using Eq. (9) provided that particles are uniformly charged.

Substituting Eq. (9) into Eq. (5), the following equation is obtained:

$$T = T_0\,\mathrm{e}^{-t/\tau} + T_\infty(1 - \mathrm{e}^{-t/\tau}) \tag{10}$$

and the saturated surface specific charge density can be estimated as

$$\sigma_\infty = \frac{\rho}{6}\frac{\int_0^\infty x^3 p(x)\,\mathrm{d}x}{\int_0^\infty x^2 p(x)\,\mathrm{d}x}T_\infty$$

The above discussion is valid for particle–wall systems that particle adhesion to the wall is negligible during the mixing process. However, particles are often found to adhere to the inner wall of mixer container with increasing mixing time, which is probably due to the enhancement of particle–wall adhesion resulting from increased electrostatic force due to charge generation and accumulation. The adhered particles form a particle layer, partially or completely coating the inner wall of the container, which modifies the surface electrical properties of the mixer wall. The coated particle layer alters particle wall charging characteristics, which is due to the change of collision between particle and particle-free wall to particle and particle-coated wall. Assuming surface coverage of the particle layer over the inner wall of the container is θ, then it is reasonable to assume that the probability of particle contact to the clean region of the wall is $1-\theta$ and the probability of particle contact to the particle-coated wall is θ. For collisions between particle and particle-coated wall, the contact potential difference is zero if the particles are of the same material. However electrostatic charge transfer may still occur because there will likely be a charge density difference between free moving and immobilized coated particles. The electrostatic charges carried by particles set up an electric field which shifts particle contact surface potential, known as image charge potential. The difference in particle surface potential shifting between free moving and coated particles resulting from their different charging densities leads to charge transfer upon collision. The charging rate of a free moving particle in this case becomes:

$$\frac{\mathrm{d}\sigma}{\mathrm{d}t} = fk_\mathrm{c}\frac{\varepsilon\varepsilon_0 S}{Z_0}\left(\frac{\phi}{\pi d^2} - k_0\sigma\right)(1-\theta) + fk_\mathrm{c}'\frac{\varepsilon\varepsilon_0 S'}{Z_0}(-k_0\Delta\sigma)\theta - k_\mathrm{r}\sigma \tag{11}$$

The first term on the right-hand side of Eq. (11) is the charge transfer due to the collision between the particle and the clean wall; the second term on the right-hand side of Eq. (11) is the charge transfer between free moving and coated particles, driven by the difference in the surface charge density; while the last term in Eq. (11) is the charge relaxation.

4. Results and discussion

Table 1 summarizes the physical properties of powder samples, which include true density, tapping density, particle size distribution, and particle aspect ratio. Morphologies of these particles were determined using SEM and are shown in Fig. A.2 (appendix). Among adipic acid, MCC, and glycine particles, the adipic acid particles had the widest particle size distribution, and MCC particles had the largest voidage which can partially be attributed to their internal pore structure. Aspect ratios (defined as the ratio of the length of the minor and the major axis) estimated based on 50 particles from SEM images were found to be 0.71 and 0.56 for adipic acid and MCC, respectively. Table 2 presents the results of particle characterization using a laser diffraction technique and image analysis for adipic acid particles composed of various size fractions obtained

Table 1
Physical characterization of particle materials

Material	True density (kg/m^3)	Tapping density (kg/m^3)	$d(0.1)$[a] (μm)	$d(0.5)$[a] (μm)	$d(0.9)$[a] (μm)	AR[b]
Adipic acid	1330	810	35.9	289.9	535.8	0.71
Glycine	1570	880	267.1	567.0	929.2	–
MCC	1560	350	83.2	142.7	236.4	0.56

[a] *Note*: $d(0.1)$, $d(0.5)$ and $d(0.9)$ stands for cumulative particle size distribution less than 10%, 50% and 90%, respectively; the particle size distribution was characterized by Malvern Mastersizer 2000 (UK) using dry mode.

[b] AR is defined as the ratio of the length of the minor and the major axis. This was characterized based on 50 images captured by SEM.

Table 2
Particle size distribution analysis by Malvern particle sizer 2000, sieve, and image analysis

Size fraction (μm)[a]	Volume size distribution by Malvern particle sizer[b]			Image analysis[c]	
	d(0.1) (μm)	*d*(0.5) (μm)	*d*(0.9) (μm)	*d*(ave) (μm)	AR
a (>500)	305.6	604.5	1130.8	588.7 ± 170.0	0.65 ± 0.14
b (250–500)	218.1	399.9	672.5	392 ± 74.6	0.62 ± 0.14
c (180–250)	97.3	223.0	395.5	279.8 ± 57.3	0.64 ± 0.17
d (150–180)	49.2	139.0	266.3	216.7 ± 38.7	0.70 ± 0.15
e (125–150)	20.7	81.0	168.7	160.7 ± 29.9	0.71 ± 0.13
f (90–125)	13.8	57.1	129.4	90.3 ± 28.1	0.71 ± 0.15

[a] These size fractions were obtained from adipic acid particles purchased from Sigma–Aldrich (refer to Table 1) through mechanical sieving.
[b] *d*(0.1), *d*(0.5) and *d*(0.9) stands for cumulative particle size distribution less than 10%, 50% and 90%, respectively; the particle size distribution was characterized by Malvern Mastersizer 2000 (UK) using dry mode.
[c] AR is defined as the ratio of the length of the minor and the major axis. This was characterized based on 50 images captured by SEM.

by a mechanical sieving. Noticeable difference in the particle size measurement by SEM image analysis and that obtained by Malvern particle sizer can be observed from Table 2. Several factors contribute to this difference. Firstly, particle size analyzed using SEM image was a projected area diameter (Fan and Zhu, 1998), while particle size obtained from Malvern particle sizer was an equivalent diameter using Mie scattering theory with a spherical model. Secondly, particle size by image analysis was number averaged from 50 SEM images. On the other hand, particle size measurement using Malvern particle sizer was volume averaged. Number-based particle size is normally smaller than volume-based particle size.

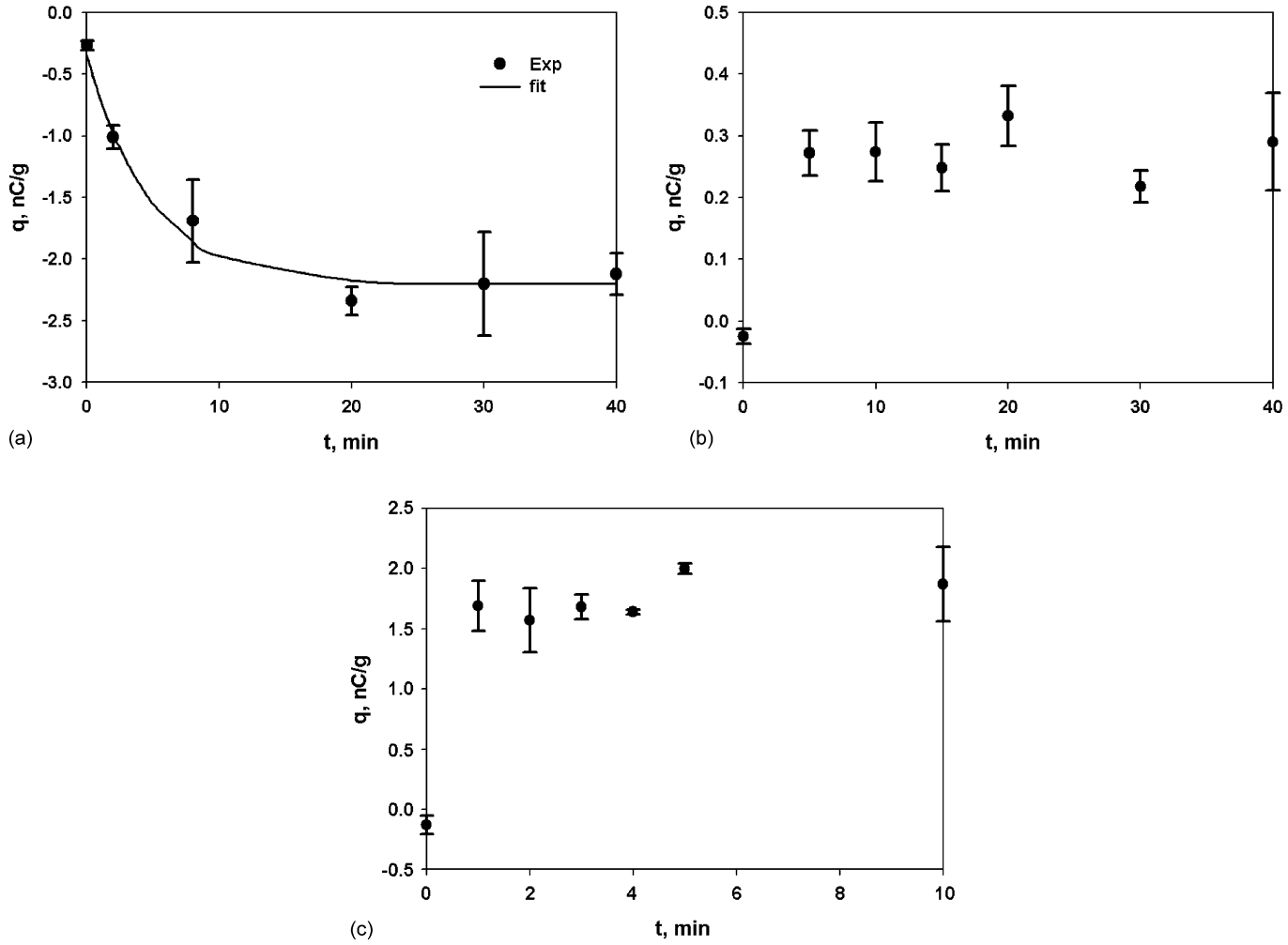

Fig. 2. Electrostatic charges acquired at various mixing time in a stainless steel container in the T2F Turbula mixer operated at the rotation speed of 49 rpm, at the temperature of 25 °C, and the relative humidity of 25% for: (a) adipic acid; (b) glycine; and (c) MCC. (●) Experimental measurement; (—) fitted with Eq. (10).

4.1. Turbula mixer

4.1.1. Charge accumulation

Fig. 2 shows the particle specific charge (q) as a function of mixing time (t) as a result of continuous impact/contact with the inner wall of the stainless steel container in the T2F Turbula mixer for adipic acid, glycine, and MCC particles at the mixer rotation speed of 49 rpm, at the temperature of 25 °C, and the relative humidity of 25%. The data and error bar was calculated using at least three independent measurements. It was found that particles acquired electrostatic charges in the mixer and the acquired charges increased with mixing time until reaching a saturated value. The saturated electrostatic charges under this investigated condition were found to be −2.2, 0.27, and 1.75 nC/g for adipic acid, glycine, and MCC particles, respectively. The saturated electrostatic charge of glycine was one order smaller than that of adipic acid and MCC particles. Experimental data for adipic acid particles were fitted quite well with Eq. (10) (solid lines in Fig. 2a) suggesting particle electrification is of first order. Compared to MCC and glycine particles, adipic acid particles were found to take longer time to be charged to the saturated value.

4.1.2. Rotation speed

Fig. 3 presents charging characteristics of adipic acid particles mixed in the stainless steel container in the T2F Turbula mixer at the temperature of 25 °C and the relative humidity of 25% with the rotation speeds of 34, 49, and 72 rpm. The corresponding saturated charge values were −2.76, −2.20, and −2.37 nC/g for 34, 49, and 72 rpm, respectively. Taking the measurement uncertainty into consideration, it appeared that the saturated electrostatic charges were not influenced by the rotation speed under the conditions investigated. Fitting the data with Eq. (10), time constants were found to decrease with increasing rotation speed—from 5.00 min for 34 rpm, 4.75 min for 49 rpm to 1.92 min for 72 rpm. This is expected since with increasing rotation speed, the frequency of impact/contact of particles with container wall increases while the interval between successive particle wall collisions for particle charge relaxation is reduced. Both effects resulted in acceleration of particle charging with increasing rotation speed. This effect was also reflected in Eq. (10).

Upon examination, fine particles were found to adhere to the container inner wall during mixing process. The mass of these adhered particles were estimated by the difference of particles loaded to and discharged from the mixer container. The percentages of particle mass loss relative to initially loaded particle mass are presented in Fig. 4 as a function of mixing time. It can be observed that around 10% of total loaded particles were found to have adhered to the inner wall of the container. These adhered particles, either forming a film layer or sparsely coating the inner wall, caused altered or partially altered particle–inner wall contacts and thereby changing the charging process. This variation could cause electrostatic charges previously acquired through particle–clean wall contacts to dissipate through "charge backflow" by free moving particles contact with adhered particles. Meanwhile, charges in the stationary particles adhered to the inner container wall may also be dissipated through charge relaxation. Both the charge relaxation and charge backflow resulted in a longer time for adipic acid particles to be charged to the saturated value than MCC and glycine particles. The particle charging kinetics in this case would not only depend on the particle wall collisions but also depend on the kinetics of the particle wall adhesion and the distribution of adhered particles inside the mixer container inner wall. This might provide the explanation for the lack of dependence of saturated particle charges on rotation speed, but this needs further investigation. The influence of adhered particles on electrostatic charging was found to be more pronounced in the horizontally oscillating mixer, and this will be discussed in a subsequent section.

4.1.3. Particle size

Fig. A.3 (appendix) shows the specific charge density acquired by adipic acid particles after mixing for 40 min in the stainless steel container attached to the Turbula mixer operated

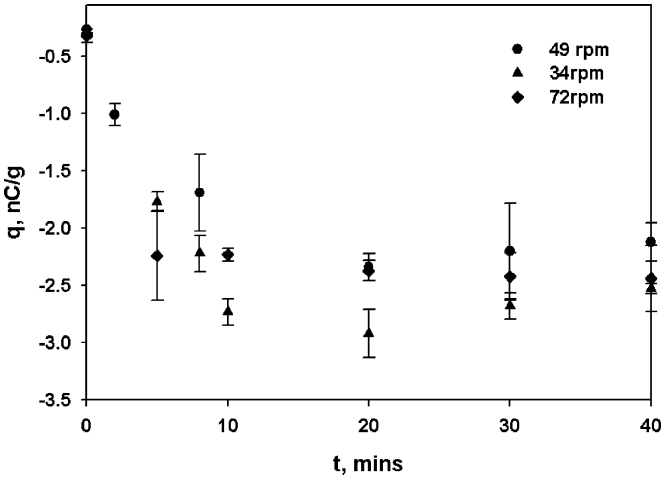

Fig. 3. Electrostatic charges acquired at various mixing time in the stainless steel container in the T2F Turbula mixer at the temperature of 25 °C and the relative humidity of 25% for adipic acid particles. The mixer rotation speeds were (●) 49 rpm; (▲) 34 rpm; and (♦) 72 rpm.

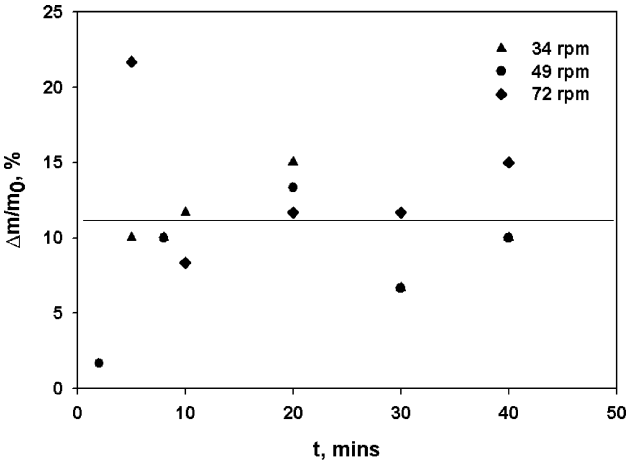

Fig. 4. Percentage of adipic acid material loss due to particle wall adhesion related to the mass of particles loaded with operating time in the stainless steel container of the T2F Turbula mixer at 25 °C and relative humidity of 25%. The rotation speeds were (●) 49 rpm; (▲) 34 rpm; and (♦) 72 rpm.

at the rotation speed of 49 rpm at the temperature of 25 °C and the relative humidity of 25% for various particle size fractions. As can be seen in Fig. 2, particles were charged to saturated values after 30 min mixing. Hence particle charges' charge levels reported in Fig. A.3 after 40 min mixing can be considered as saturated electrostatic charges. The particle fractions correspond to those in Table 2. As discussed earlier, particle charge mass ratio would be inversely proportional to the particle diameter if the surface charge density was the same for all particle samples. However, no apparent dependence of specific particle charge on average particle size was found for adipic acid particles in the present investigation. This suggested that specific charge densities may not be the same for particles of different size fractions.

For particle samples not having very narrow particle size distribution as those used in the present work, surface specific charge density, as opposed to mass specific charge density, may be a better indicator to describe particle tribo-electrification process (Chen, 1974). Fig. 5 shows the surface specific charge density after mixing 40 min for various particle size fractions at the rotation speeds of 49, 72, 101 rpm, at the temperature of 25 °C, and the relative humidity of 25%. It was found that surface specific charge densities increased with increasing particle size for particle size fraction *d* to *a*. However there were little differences in surface specific charge densities for particles of size fractions *d*, *e* and *f*.

Fig. 6 shows the percentage particle mass loss related to the initial particle mass loaded for adipic acid particles due to particle adhesion to the inner wall after mixing 40 min in the container for various particle size fractions rotated at 49, 72, and 101 rpm, with the temperature of 25 °C and the relative humidity of 25%. It can be seen that for all particle size fractions there were some adipic acid particles adhering to the inner wall. Taking the measurement uncertainty into account, the particle mass losses were almost the same for particles of size fraction *a* to *d* and increased with decreasing particle size from size fraction *d* to *f*. The percentages of mass loss were found to be few percent for particles

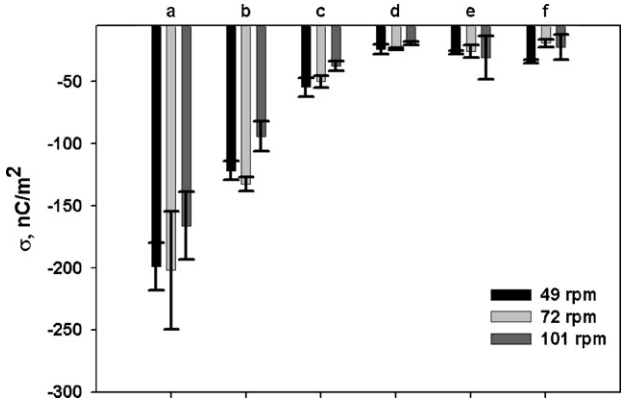

Fig. 5. Surface specific charge density of adipic acid particles in the stainless steel container of the T2F Turbula mixer after mixing at the rotation speed of 49, 72, and 101 rpm for 30 min at the temperature of 25 °C and the relative humidity of 25% for various particle size fractions. The detail information for the characteristics of adipic acid particles for various size fractions can be found in Table 2.

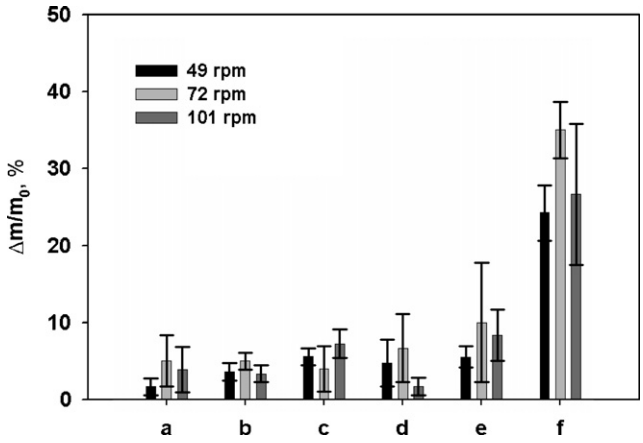

Fig. 6. Percentage of material loss related to the mass of particles loaded due to sticking onto the inner wall of the stainless steel container of the T2F Turbula mixer at the temperature of 25 °C and the relative humidity of 25% with rotation speed of 49, 72, and 101 rpm for adipic acid particles of various particle size fractions. The detail information for the characteristics of adipic acid particles for various size fractions can be found in Table 2.

of large size fractions to a few tens percent for the particles of small size fractions. For a specific container with an inner wall area A_w, and particle mass loss m_a as a result of adhesion, and the number probability $p(d)$ for particles having size d, if monolayer particle adhesion is assumed, total projection area of adhered particle A_T is

$$A_T = \sum n_i A_i = N \int_{a_1}^{a_2} p(a)\pi a^2 \, da \tag{12}$$

where N is the total number of adhered particles, which can be calculated as follows:

$$N = \frac{m_a}{\int_{a_1}^{a_2} (1/6)\pi a^3 p(a)\rho \, da} \tag{13}$$

Then particle coverage θ can be estimated as follows:

$$\theta = \frac{A_T}{A_w} = \frac{m_a}{A_w} \frac{\int_{a_1}^{a_2} \pi a^2 p(a) \, da}{\int_{a_1}^{a_2} (1/6)\rho p(a)\pi a^3 \, da} \tag{14}$$

It follows from Eq. (14) that the coverage of particles over the inner container wall due to the adhered particles increased with the mass of particle loss for specific particle size; and for a certain amount mass of particle loss, the coverage of particle over the inner wall was increased with decreasing particle size. It thus can be concluded from Fig. 6 that particle coverage on the inner container wall arising from the adhesion of adipic acid particles increased with decreasing particle size. The layer of adhered particle altered the particle wall contact from particle–wall contacts to particle-adhered particle contacts. This further influenced the particle electrification process. This effect appeared to be more pronounced for particles of smaller size fractions.

For adipic acid particles of larger size fractions (*a*, *b*, *c*, *d*), surface specific charge density increased with increasing particle size. Two factors may contribute to this observation. Firstly, bigger particles experienced larger deformation as a result of higher impact velocity associated with larger inertia in the mixer, which resulted in larger charge transfer (Matsusaka et al., 2000; Ema

et al., 2003). Secondly, coverage of particles over the inner wall of container was lower for bigger particles as discussed earlier. Particle coverage over inner container wall resulted in charge "backflow" through particle colliding with particle-coated wall as discussed earlier. The lower particle surface coverage of the inner container wall had led to smaller charge "backflow" as discussed and also demonstrated in Eq. (11). Both effects resulted in bigger particles having larger specific surface charge densities. For particles of smaller size fractions (*d*, *e*, *f*), specific charge densities were found to be more or less the same. This could be due to the ease of contact between free moving particles and adhered particles. Effects of surface modification of particle processing devices on particle charging were also reported by Eilbeck et al. (2000) and Murtomaa et al. (2004). Dependence of specific surface charge density was found to be directly proportional to particle size (averaged particle size). This indicated that particle charge was proportional to particle size raised to the powder of 3. Surface specific charge densities were found to be almost the same for particles mixed at different rotation speeds in the stainless steel container. This is consistent with the charge accumulation process shown in Fig. 3.

4.1.4. Relative humidity

Particles will adsorb/desorb moisture from the surroundings if exposed to a higher/lower relative humidity environment. The presence of moisture residues at the surface of particles can alter the conductivity of powder mass, and thereby varying particle charging characteristics. Adipic acid material and MCC particles were employed to investigate the equilibrium charge values at 25 °C and the relative humidity from 25% to 85%. Dynamic Vapor Sorption analysis (DVS: SMS, UK) revealed that unsieved adipic acid material was not hygroscopic at 25 °C. The moisture sorption curve for MCC by DVS is presented in Fig. 7. Water content for monolayer coverage was found to be around 4% (w/w) at the corresponding relative humidity of about 25%. The

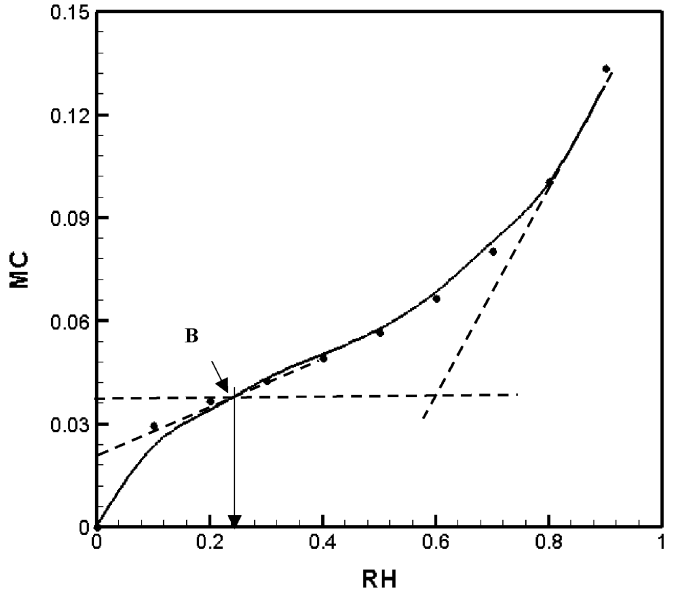

Fig. 7. Adsorption isotherm of moisture by MCC powders at 25 °C. (●) Experimental; (—) GAB model. Point "B" characterizing monolayer moisture content.

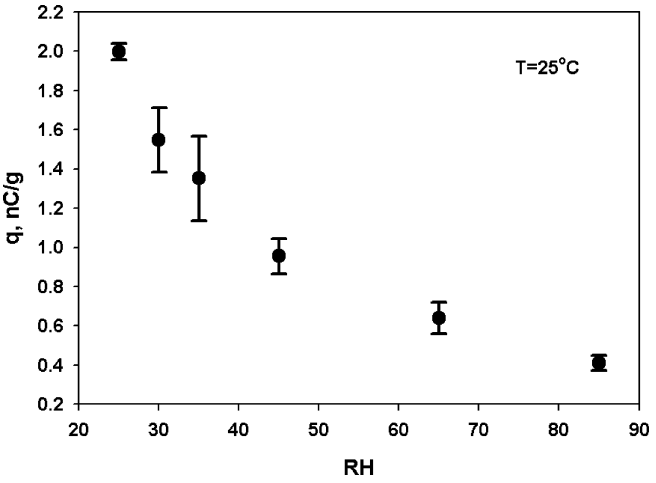

Fig. 8. Specific charge density of MCC particles acquired in the stainless steel container of the T2F Turbula mixer operated at the rotation speed of 49 rpm and the temperature of 25 °C for various relative humidity from 25% to 85%.

mixing times used were 15 and 40 min for MCC and adipic acid particles, respectively, to ensure that the particles were fully charged. It was found that under the conditions investigated the influence of relative humidity on the adipic acid particle charging was negligible. Fig. 8 presents the saturated electrostatic charges of MCC particles over various relative humidity at the temperature of 25 °C. Unlike adipic acid particles, MCC particles were found to be having a higher saturated static charge values at lower relative humidity.

4.2. Horizontally oscillating mixer

4.2.1. Particle charging

In addition to the Turbula mixer, particle charging in another type of mixer, a horizontally oscillating mixer, was also investigated for various particles in the controlled environment. The mixer was operated at the frequency of 2.5 Hz under the same environment as the Turbula mixer, that is, the temperature of 25 °C and the relative humidity of 25%. Fig. 9 presents the kinetics of electrostatic charging processes in the mixer for adipic acid, MCC and glycine particles, respectively, and the corresponding saturated electrostatic charges were -3.67 ± 0.48, 2.71 ± 0.33, and 3.85 ± 0.12 nC/g. Like particle electrification in the Turbula mixer, adipic acid particles acquired negative charges, and MCC as well as glycine particles obtained positive charges in the horizontal oscillating mixer. However, the magnitudes of equilibrium particle charges were much larger in the horizontally oscillating mixer compared to those in the Turbula mixer, especially for glycine particles. The increase in the equilibrium particle electrostatic charges could be caused by difference in particle–mixer relative motion in mixer. In the Turbula mixer particles experienced rotation, translation, and inversion motions whilst in the horizontally oscillating mixer particles mainly slide against the wall. This sliding frictional motion caused an increase in the apparent contact area and resulted in an increase in the particle charging compared to impact dominant charging process. The observations that particles were more charged by the sliding motion than in direct impact are in agree-

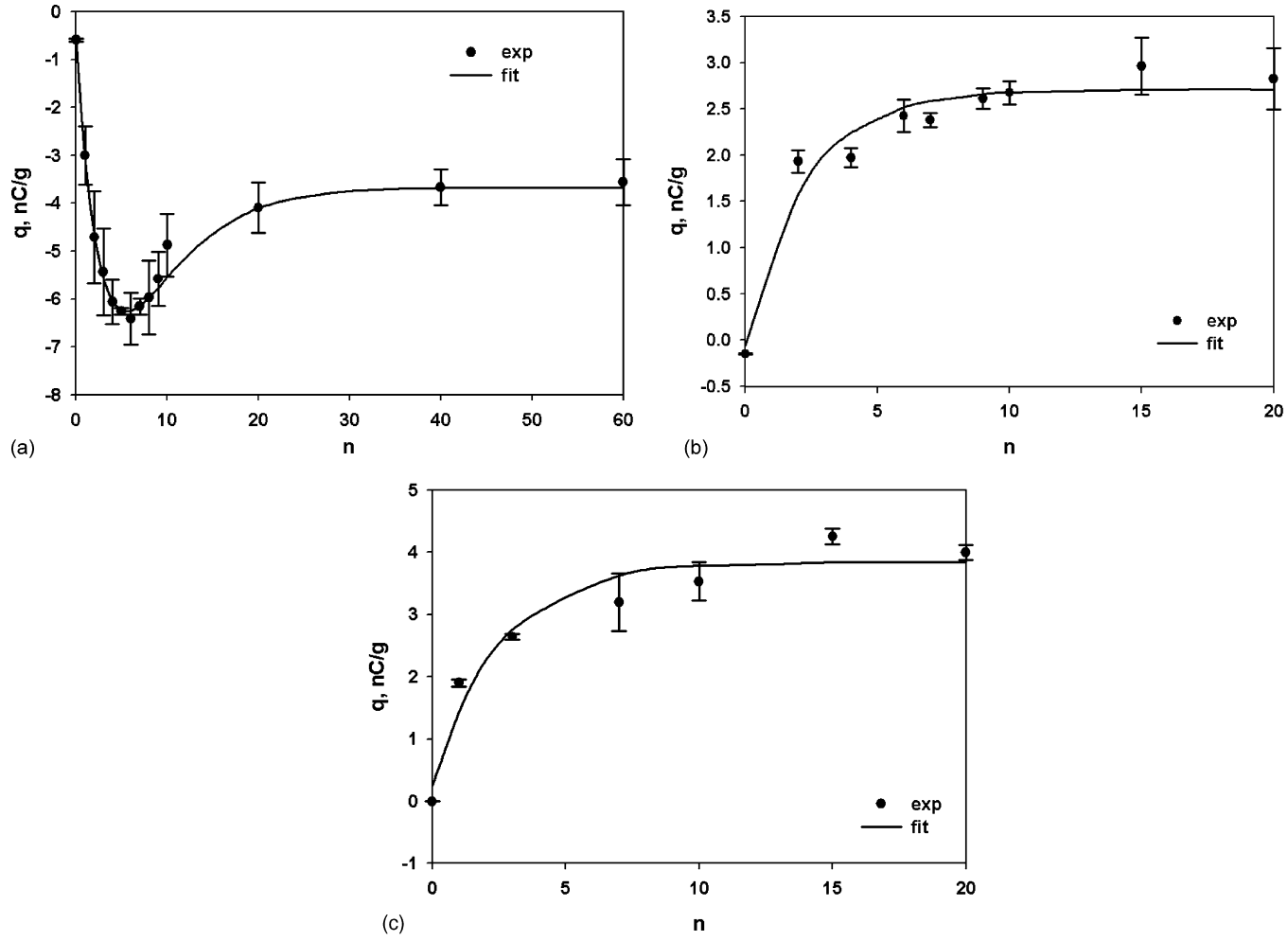

Fig. 9. Electrostatic charges acquired at various operating time in a stainless steel container of the horizontally oscillating mixer at the temperature of 25 °C and the relative humidity of 25% for various particles: (a) adipic acid; (b) MCC; (c) glycine. (●) Experimental measurement; (—) fitted with two-exponential equation for (a) and Eq. (10) for (b) and (c).

ment with previously reported research work (Yoshida et al., 2003; Ema et al., 2003).

Charge accumulation processes for MCC and glycine particles in the horizontally oscillating mixer were found to follow similar trends as those in the Turbula mixer where particle electrostatic charges increased with time until they reached saturated values. Time constants for the horizontally oscillating mixer were found to be 2.3 and 2.5 cycles for MCC and glycine, respectively. However, very different charging process was observed for adipic acid in the horizontally oscillating mixer. It was found that adipic acid particles firstly acquired negative electrostatic charges rapidly upon onset of the mixing operation, reached a maxima of about −6.5 nC/g around 7 cycles, after which particle acquired charges started to dissipate, and finally equilibrated at around −3.7 nC/g after 40 cycles. The data obtained were well fitted with a double-exponential function (Ohara, 1988) with the time constants of $\tau_1 = 3.2$ and $\tau_2 = 5.7$ cycles, respectively. Time constant $\tau_1 = 3.2$ for adipic acid was comparable with 2.3 for MCC and 2.5 for glycine. The time constant $\tau_2 = 5.7$ suggested that another slower process could be simultaneously affecting the particle charging process for adipic acid.

Fig. 10 shows the mass loss with time due to particle–wall adhesion for adipic acid, glycine and MCC particles in the horizontally oscillating mixer at the temperature of 25 °C and the relative humidity of 25%. It can be observed that mass losses for MCC and glycine particles were negligible, similar to the case of Turbula mixer. However, mass loss for adipic acid particles as a result of particles adhering to the inner container wall increased with mixing time and the percentage of mass loss relative to particle mass initially loaded was as high as 50% after 40 cycles.

The different charging characteristics may be attributed to this difference in particle–wall adhesion behavior. As discussed earlier with respect to particle charging in the Turbula mixer, MCC and glycine particles collided directly with stainless steel wall causing charges to be generated and accumulated to an equilibrium value as described by Eq. (10). However, for the case of adipic acid, particle wall adhesion was found to be present in the mixing process, affected by the particle size and enhanced by the electrostatic charges. Meanwhile, particle wall adhesion modified the particle wall contact behavior, and thereby particle electrification process. The mutual interaction of particle

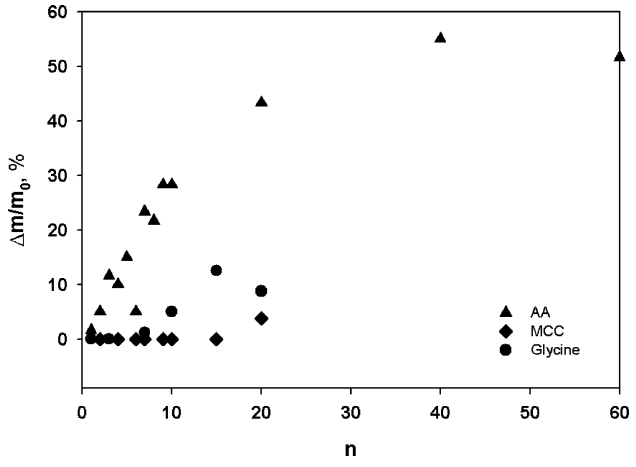

Fig. 10. Percentage of material loss related the mass of particles loaded with operating time due to particles adhering to the inner wall of stainless steel container of the horizontally oscillating mixer at the temperature of 25 °C and the relative humidity of 25% for (●) glycine; (▲) adipic acid; and (♦) MCC.

charging and wall adhesion resulted in rapid particle electrostatic charge generation and accumulation at the onset of mixing operation, followed by slow charge dissipation, and finally arrived at the equilibrium value (Fig. 9a). This kind charging behavior can be described using Eq. (11). Mutual interaction of particle charging and wall adhesion led to the first order increase in the particle losses due to the wall adhesion as shown in Fig. 10.

4.2.2. Particle size

Compared to adipic acid particles, the mass losses of MCC and glycine particles were negligible. The relative magnitudes of removal and adhesion forces determined whether particles would adhere to the wall or not. The removal force was associated with particle inertia, which was directly proportional to d^3. The particle wall adhesion force composed mainly of van der Waals and electrostatic forces if water capillary force was negligible. The van der Waals attraction force was proportional to particle diameter according to the JKR model (Johnson et al., 1971), and in the absence of external electrical field the electrostatic force on a charged particle contact with electrically conducting substrate was directly proportional to q^2 and inversely proportional to d^2 (Feng and Hays, 2003). If assuming that surface specific charge density did not depend on particle size and the particle was spherical, the electrostatic force was in effect proportional to the diameter square (d^2). This analysis suggested that if surface specific charge density was constant (particle size independent), particles having smaller size would tend to adhere to the wall more readily. Therefore adipic acid adhesion to the wall could be eliminated if the particle size was larger enough, and the corresponding charging behavior would be different.

To verify the above analysis of particle size effect on particle wall adhesion and hence particle electrification, adipic acid particle samples of different size fractions were obtained for investigations in the horizontally oscillating mixer under the same operational condition and experimental environment. Fig. 11(a) presents the particle mass loss arising from particle adhesion to

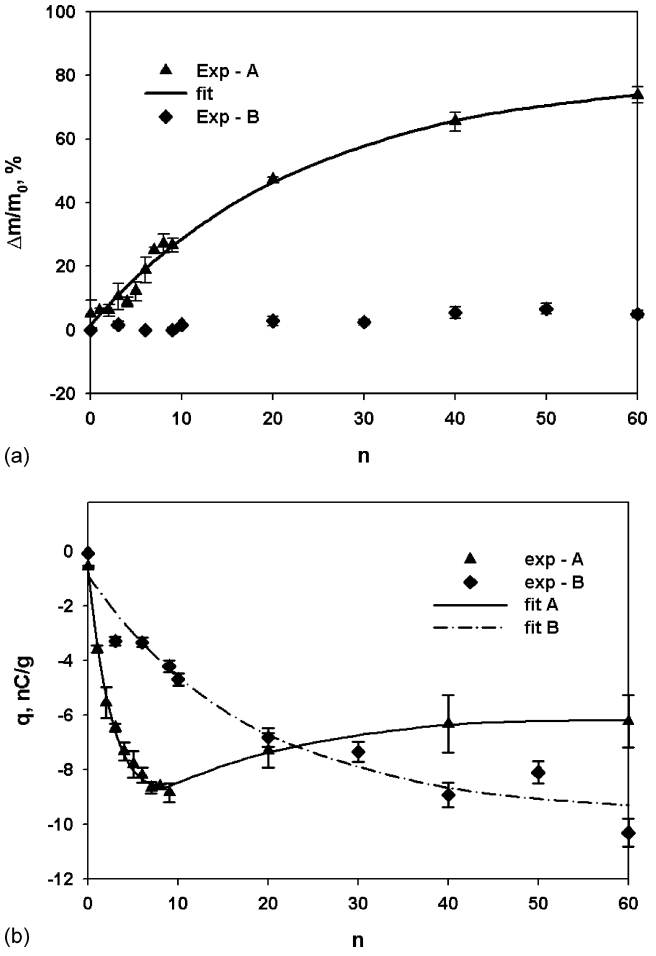

Fig. 11. Electrification of adipic acid particles with two different size fractions in the horizontally oscillating mixer operated at the temperature of 25 °C and the relative humidity of 25%. (a) Percentage of material loss related to the mass of particles loaded; (b) particle electrification kinetics. (▲) Adipic acid particles of size fraction 150–180 μm; (♦) adipic acid particles of size fraction larger than 500 μm; (—) fitted with two-exponential equation; (—) fitted with Eq. (10).

the wall for the two different size fractions, namely size fractions *a* and *e* as shown in Table 2. As expected, it can be clearly seen that in the case of larger particles, size fraction *a* in Table 2, there was indeed no noticeable particle loss in the first 10 cycles and negligible particle loss over the next 50 cycles (less than 4%). In the case of smaller particles (size fraction *e* in Table 2), adipic acid particles were found to adhere appreciably to the inner wall of mixer container and the adhesion particle mass loss was found to increase with mixing cycles up to a saturated value of about 70% at 60 cycles. Fig. 11(b) shows the corresponding specific particle charge measurements at different mixing cycles for the two different size fractions. Adipic acid particle of size fraction *a* in Table 2 acquired electrostatic charges with increased mixing cycles until reaching a saturated value of around −10 nC/g and exhibited the same trend as those for MCC and glycine particles albeit of negative polarity. However, smaller adipic acid particles (size fraction *e* shown in Table 2) firstly acquired static charges rapidly, then reached a maximum value around −9 nC/g, and finally equilibrated at a smaller saturated value of −6 nC/g. This particle electrification behavior was similar to that of unsieved

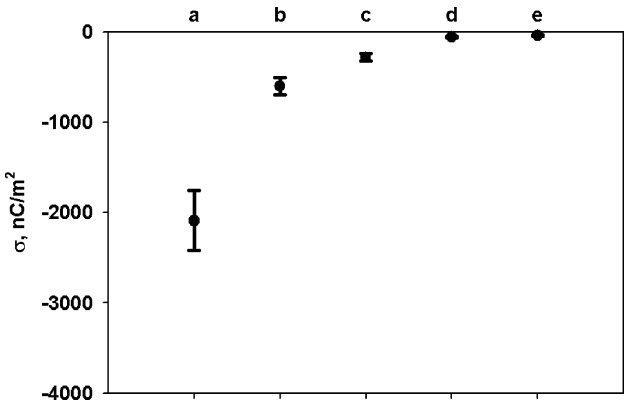

Fig. 12. Surface specific charge density after mixing for 60 cycles in the horizontally oscillating stainless steel mixer for adipic acid particles of various size fractions. The detail information for the characteristics of adipic acid particles for various size fractions can be found in Table 2.

adipic acid materials. This observation confirmed that different charging characteristics of unsieved adipic acid material and fine adipic acid fraction, compared to coarse adipic acid fraction, MCC and glycine, were indeed due to adhesion of particles onto the mixer container wall.

Fig. 12 shows the surface specific charge density measured at the temperature of 25 °C and the relative humidity of 25% for various particle size fractions of adipic acid particles. It showed that the surface specific charge density was larger for larger particles. This observation was also consistent with the findings in the Turbula mixer.

5. Conclusions

The electrification behaviors of adipic acid, MCC, and glycine particles in the Turbula and horizontally oscillating mixers were measured using a Faraday cage. The influence of rotation speed, particle size distribution, mixer type and relative humidity on particle charging characteristics were investigated. Conclusions obtained from the current work are summarized in the following point form:

(1) Unsieved and fine adipic acid particles were found to stick to the inner wall of the mixer container and the amount in particles adhering on the wall increased with mixing time. The increase in the amount of particles adhering on the wall was due to enhanced particle wall adhesion arising from the increase in electrostatic force.
(2) The level of adhered particles covering the inner wall of mixer container can proportionally alter the particle–wall contacts to particle-adhered particle contacts, which caused particle charge to increase initially with mixing time then decrease to a smaller saturated value with additional mixing time.
(3) The charging profiles for unsieved and fine adipic acid particles were different from those of coarse adipic acid, MCC and glycine particles where particle charge increased monotonically with mixing time until reaching to saturated charge levels. This difference in charging kinetics was due to the presence of particles adhering to the inner wall of mixer containers.
(4) Specific surface charge densities were found to increase with increasing particle size for larger particle size fractions and more or less constant for smaller particle size fractions. These size dependent specific surface charge densities were believed to be due to the combined effects of both particle inertia and particle wall coverage.
(5) Mass loss of particles due to particle wall adhesion was found to be negligible for MCC and glycine particles. MCC and glycine particles were found to be charged to the saturated charge values much faster than adipic acid particles, and the difference in charging kinetics was believed to be due to the presence of adhered particles at the mixer inner container wall.
(6) Fine particles may be lost through particle wall adhesion in the mixer when mixing fine and coarse particle together, for example, during mixing of fine drug particles and larger carrier particles in dry powder inhalation formulation developments. The results obtained from current work can be useful as a guide for possible consequences during particle mixing operations.

Particle electrification in the mixer reported in this study can be used to quantify the electrostatic charge interactions between pharmaceutical powders and equipment surfaces. The interactions provide information regarding the behavior of pharmaceutical powders. The inter-play between particle electrostatic charge and particle wall adhesion as discussed in this work are relevant to many pharmaceutical operations. Data of charge propensity of pharmaceutical powders to appropriate contact surfaces is very useful for formulation and processing engineering in the design and manufacture of pharmaceutical operation systems.

Acknowledgements

The authors would like to thank A-STAR (Agency for Science, Technology and Research of Singapore) for providing financial support for this project (in house project ICES/05-422001). The authors would also like to thank Ms. Wei Xiaohong (Nanyang Technological University) for her help in the electrostatic charge measurement experiments, Ms. Chew Jia Wei for providing Glycine samples, Mr. Kwek Jin Wang for analyzing particle morphology, and Ms. Chew Meizeng for her help during this study.

Appendix A. Supplementary data

Supplementary data associated with this article can be found, in the online version, at doi:10.1016/j.ijpharm.2006.07.041.

References

Bailey, A.G., Smedley, C.J.A., 1991. Impact charging of polymer particles. Adv. Powder Technol. 2, 277–284.

Byron, P.R., Peart, J., Staniforth, J.N., 1997. Aerosol electrostatics. I. Properties of fine powders before and after aerosolization by dry powder inhalers. Pharm. Res. 14, 698–705.

Carter, P.A., Cassidy, O.E., Rowley, G., Merrifield, D.R., 1998. Triboelectrification of fractionated crystalline and spray-dried lactose. Pharm. Pharmacol. Commun. 4, 111–115.

Castle, G.S.P., Schein, L.B., 1995. General model of sphere–sphere insulator insulator contact electrification. J. Electrostat. 36, 165–173.

Chen, A.H., Bi, H.T., Grace, J.R., 2003. Measurement of particle charge-to-mass ratios in a gas–solids fluidized bed by a collision probe. Powder Technol. 135, 181–191.

Chen, I., 1974. Statistics of charged powder particles. J. Appl. Phys. 45, 4852–4856.

Clint, J.H., Dunstan, T.S., 2001. Acid–base components of solid surfaces and the triboelectric series. Europhys. Lett. 54, 320–322.

Diaz, A.F., Felix-Navarro, R.M., 2004. A semi-quantitative tribo-electric series for polymeric materials: the influence of chemical structure and properties. J. Electrostat. 62, 277–290.

Diaz, A.F., Fenzel-Alexander, D., 1993. An ion transfer model for contact charging. Langmuir 9, 1009–1015.

Dubus, J.C., Guillot, C., Badier, M., 2003. Electrostatic charge on spacer devices and salbutamol response in young children. Int. J. Pharm. 261, 159–164.

Eilbeck, J., Rowley, G., Carter, P.A., Fletcher, E.J., 2000. Effect of contamination of pharmaceutical equipment on powder triboelectrification. Int. J. Pharm. 195, 7–11.

Eliasen, H., Kristensen, H.G., Shafer, T., 1999. Electrostatic charging during a melt agglomeration process. Int. J. Pharm. 184, 85–96.

Elsdon, R., Mitchell, F.R.G., 1976. Contact electrification of polymers. J. Phys. D: Appl. Phys. 9, 1445–1460.

Ema, A., Yasuda, D., Tanoue, K., Masuda, H., 2003. Tribo-charge and rebound characteristics of particles impact on inclined or rotating metal target. Powder Technol. 135–136, 2–13.

Fan, L.S., Zhu, C., 1998. Principles of Gas–Solid Flows. Cambridge University Press.

Feng, J.Q., Hays, D.A., 2003. Relative importance of electrostatic forces on powder particles. Powder Technol. 135–136, 65–75.

Guardiola, J., Rojo, V., Ramos, G., 1996. Influence of particle size, fluidization velocity and relative humidity on fluidized bed electrostatics. J. Electrostat. 37, 1–20.

Harper, W.R., 1967. Contact and Frictional Electrification. Oxford University Press, UK.

Hendrickson, G., 2006. Electrostatics and gas phase fluidized bed polymerization reactor wall sheeting. Chem. Eng. Sci. 61, 1041–1064.

Johnson, K.L., Kendall, K., Robberts, A.D., 1971. Surface energy and the contact of elastic solid. Proc. Roy. Soc. A 324, 301–313.

Jones, T.B., 1995. Electromechanics of Particles. Cambridge University Press, Cambridge.

Joseph, S., Klinzing, G.E., 1983. Vertical gas–solid transition flow with electrostatics. Powder Technol. 36, 79–87.

Kanagy II, S.P., Mann, C.J., 1994. Electrical properties of eolian sand and silt. Earth-Sci. Rev. 36, 181–204.

Kanazawa, S., Ohkubo, T., Nomoto, Y., Adachi, T., 1995. Electrification of a pipe wall during powder transport. J. Electrostat. 35, 47–54.

Kleber, W., Makin, B., 1998. Triboelectric powder coating: a practical approach for industrial use. Part. Sci. Technol. 16, 43–53.

Kulvanich, P., Stewart, P.J., 1987. Correlation between total adhesion and charge decay of a model interactive system during storage. Int. J. Pharm. 39, 51–57.

Kwok, P.C.L., Glover, W., Chan, H.K., 2005. Electrostatic charge characteristics of aerosol produced from metered dose inhalers. J. Pharm. Sci. 94, 2789–2799.

Lee, L.H., 1994. Dual mechanism for metal–polymer contact electrification. J. Electrostat. 32, 1–29.

Masuda, H., Komatsu, T., Iinoya, K., 1976. The static electrification of particles in gas–solids pipe flow. AIChE J. 22, 558–564.

Masuda, H., Matsusaka, S., Shimomura, H., 1998. Measurement of mass flow rate of polymer powder based on static electrification of particles. Adv. Powder Technol. 9, 169–179.

Matsusaka, S., Ghadiri, M., Masuda, H., 2000. Electrification of an elastic sphere by repeated impacts on a metal plate. J. Phys. D: Appl. Phys. 33, 2311–2319.

Matsusaka, S., Nishida, T., Gotoh, Y., Masuda, H., 2003. Electrification of fine particles by impact on a polymer film target. Advanced Powder Technol. 16 (1), 127–138.

Matsuyama, T., Yamamoto, H., 1995. Electrification of single polymer particle by successive impacts with metal targets. IEEE Trans. Ind. Appl. 31 (6), 1441–1445.

Matsusyama, T., Yamamoto, H., 2006. Impact charging of particulate materials. Chem. Eng. Sci. 61, 2230–2238.

Murtomaa, M., Mellin, V., Harjunen, P., Lankinen, T., Laine, E., Lehto, V.P., 2004. Effect of particle morphology on the triboelectrification in dry powder inhalers. Int. J. Pharm. 282, 107–114.

Ohara, K., 1988. A method of exponential function analysis of contact and frictional electrification curves. J. Electrostat. 20, 319–326.

Philip, V.A., Mehta, R.C., Mazumder, M.K., DeLuca, P.P., 1997. Effect of surface treatment on respirable fractions of PLGA microspheres formulated for dry powder inhalers. Int. J. Pharm. 151, 165–174.

Rasanen, E., Rantanen, J., Mannermaa, J.P., Yliruusi, J., 2004. The characterization of fluidization behavior using a novel multichamber microscale fluid bed. J. Pharm. Sci. 93, 780–791.

Rosales, C., Sanderson, M.L., Hemp, J., 2002. Problems in the theory and design of electromagnetic flowmeters for dielectric liquids. Part2b. Theory of noise generation by charged particles. Flow Meas. Instrum. 13, 165–171.

Yanar, D.K., Kwetkus, B.A., 1995. Electrostatic separation of polymer powders. J. Electrostat. 35, 257–266.

Yoshida, M., Shimosaka, A., Shirakawa, Y., Hidaka, J., Matsuyama, T., Yamamoto, H., 2003. Estimation of electrostatic charge distribution of flowing toner particles in contact with metals. Powder Technol. 135–136, 23–34.

Yu, Z.Z., Watson, K., 2001. Two-step model for contact charge accumulation. J. Electrostat. 51–52, 313–318.

Zeng, X.M., Martin, G.P., Tee, S.K., Ghoush, A.A., Marriott, C., 1999. Effects of particle size and adding sequence of fine lactose on the deposition of salbutamol sulphate from a dry powder formulation. Int. J. Pharm. 182, 133–144.

Zheng, X.J., Huang, N., Zhou, Y., 2006. The effect of electrostatic force on the evolution of sand saltation cloud. Eur. Phys. J. E 19, 129–138.

Zheng, X.J., Huang, N., Zhou, Y.H., 2003. Laboratory measurement of electrification of wind-blown sands and simulation of its effect on sand saltation movement. J. Geophys. Res. 108, 4322–4331.

Zhu, K.W., Rao, S.M., Huang, Q.H., Wang, C.H., Matsusaka, S., Masuda, H., 2004. On the electrostatics of pneumatic conveying of granular materials using electrical capacitance tomography. Chem. Eng. Sci. 59, 3201–3213.